AIP | Journal of Applied Physics

Exploiting magnetic asymmetry to concentrate diamagnetic particles in ferrofluid microflows

James J. Wilbanks, Garrett Kiessling, Jian Zeng, Cheng Zhang, Tzuen-Rong Tzeng, and Xiangchun Xuan

Citation: Journal of Applied Physics **115**, 044907 (2014); doi: 10.1063/1.4862965
View online: http://dx.doi.org/10.1063/1.4862965
View Table of Contents: http://scitation.aip.org/content/aip/journal/jap/115/4?ver=pdfcov
Published by the AIP Publishing

Exploiting magnetic asymmetry to concentrate diamagnetic particles in ferrofluid microflows

James J. Wilbanks,[1] Garrett Kiessling,[1] Jian Zeng,[1] Cheng Zhang,[2] Tzuen-Rong Tzeng,[3] and Xiangchun Xuan[1,a)]
[1]*Department of Mechanical Engineering, Clemson University, Clemson, South Carolina 29634-0921, USA*
[2]*Department of Mechanical Engineering, Georgia Southern University, Statesboro, Georgia 30460, USA*
[3]*Department of Biological Sciences, Clemson University, Clemson, South Carolina 29634-0314, USA*

(Received 22 October 2013; accepted 9 January 2014; published online 27 January 2014)

Concentrating particles and cells for measurement or removal is often essential in many chemical and biological applications. Diamagnetic particle concentration has been demonstrated in magnetic fluids using two repulsive or attracting magnets, which in almost all cases are symmetrically positioned on the two sides of the particle-flowing channel. This work studies the effects of magnet asymmetry on the pattern and flow rate of diamagnetic particle concentration in ferrofluid flow through a straight rectangular microchannel. Two attracting permanent magnets with a fixed distance are each embedded on one side of the microchannel with a symmetric or an asymmetric configuration. A pair of symmetric counter-rotating circulations of concentrated particles is formed in the microchannel with a symmetric magnet configuration, which is found to grow in size and progress up the flow. In contrast, the single asymmetric circulation of concentrated particles formed in the microchannel with an asymmetric magnet configuration nearly maintains its size and position. Moreover, the magnet asymmetry is found to increase the ferrofluid flow rate for particle trapping, which is predicted by a three-dimensional theoretical model with a reasonable agreement.
 [http://dx.doi.org/10.1063/1.4862965]

I. INTRODUCTION

In many fields, such as environmental monitoring, food safety, medicine, and water quality control, it is necessary to concentrate particles and cells to allow for their detection and analysis.[1] Numerous physical mechanisms have been proposed and investigated to trap and enrich particles in microfluidic devices.[2] These methodologies are usually classified as surface contact or contactless methods based on the physical principle utilized in the device.[3] Surface contact-based methods include hydrodynamic trapping with microchannel geometry,[4] trapping by chemical bonding,[5] and trapping using microfilters.[6] These methods are costly in terms of experimental preparation and execution, and are typically limited by the compatibility of the method with the dimensions or physical properties of only one particle type.

Non-contact methods to immobilize particles utilize force fields to manipulate the particle motion in the suspending fluid,[1–3] and benefit from reversible trapping by controlling the driving field. Optical methods have been investigated to control the electrokinetic patterning of particles,[7] remove particles and cells from a microfluidic flow utilizing a micrometer scale optical fiber,[8] and trap particles and cells with optoelectronic tweezers,[9] etc.[10] Acoustic field-based techniques have been demonstrated to trap particles and cells in disposable rectangular borosilicate capillaries with a standing ultrasonic wave created by a piezoelectric transducer,[11] and pattern particles and cells in one- and two-dimensional arrangements using standing surface acoustic waves, etc.[12] Electric field can also be used to concentrate particles through primarily dielectrophoresis (DEP), the motion of particles in response to a non-uniform electric field.[13] Positive DEP (pDEP) and negative DEP (nDEP) have both been utilized in microfluidic devices to concentrate various micron- and nano-sized particles, where particles are attracted to regions of high electric field in pDEP and repelled from these areas in nDEP.[14] The electric field gradients can be created by placing an insulating material between two electrodes[15,16] or by an array of electrodes.[17]

Another significant methodology used to trap and concentrate particles is the utilization of magnetic field, which has several advantages over other force-driven methods, including simple, low-cost, and free of heating issues, etc.[18–20] Traditionally, magnetic field has been long used to concentrate magnetic particles through positive magnetophoresis, where the particles are pulled towards the source of the magnetic field.[21,22] However, the majority of the particles encountered in our life is diamagnetic (or non-magnetic as often called), and hence needs to be artificially tagged with magnetic particles in order for magnetic manipulation.[18–22] Label-free magnetic concentration of diamagnetic particles can be implemented through negative magnetophoresis, where particles suspended in a magnetic fluid are repelled away from the source of magnetic field. This has been demonstrated in ferrofluids[23–26] and paramagnetic solutions (e.g., $MnCl_2$)[27–29] through the use of micro-patterned magnets,[25,26] which is complicated, or simply two interacting permanent magnets.[23,24,27–29] In the latter, the two magnets can be repelling with their like poles facing each other, under which diamagnetic particles are trapped between the magnets.[23,24,27] Alternatively, the two magnets can be attracting

a)Author to whom correspondence should be addressed. Electronic mail: xcxuan@clemson.edu. Fax: 864-656-7299.

with their opposite poles facing each other, under which diamagnetic particles are concentrated outside the facing surfaces of the magnets.[28,29] In all these works, the two repelling or attracting magnets have a symmetric configuration with respect to the particle-flowing channel.

Our group has recently developed a simple diamagnetic particle concentration technique in a ferrofluidic microchip using two attracting permanent magnets placed on the top and bottom of the planar device.[30] In contrast to those works as reviewed above, the two magnets were positioned asymmetrically with respect to the microchannel. Two stable counter-rotating circulations or random wave-like motions were observed for the concentrated particles, which were speculated to be associated with the asymmetric magnet configuration. This work is aimed to investigate the effects of magnet asymmetry on diamagnetic particle concentration in ferrofluid flow through a straight rectangular microchannel. Two permanent magnets are embedded into the polydimethylsiloxane (PDMS) of the ferrofluidic microchip with their opposite pole surfaces facing each other, i.e., attracting. The maximum ferrofluid flow rate for particle trapping and the development of particle concentration are examined and compared in the microchannels with symmetric and asymmetric magnet configurations, respectively. A three-dimensional theoretical model is also developed to simulate the transport and trapping of diamagnetic particles in ferrofluid microflows.

II. EXPERIMENT

A. Microfluidic device fabrication

The microchannels utilized in the experiments were straight rectangular microchannels with a depth of 60 μm, a length of 2 cm, and a width of 600 μm. They were fabricated using the standard soft-lithography method. First, photoresist (SU-8 25, MicroChem Corporation, Newton, MA) was distributed on a clean glass slide, which was placed in a spin coater (WS-400E-NPP-Lite, Laurell Technologies, North Wales, PA) for coating at a terminal velocity of 800 rpm. Next, the glass slide was baked on a hot plate (HP30A, Torrey Pines Scientific, San Marcos, CA) at 65 °C for a period of 7.25 min and at 95 °C for an additional 22.75 min. Then, a photomask with the channel design printed on a transparent film was placed on the photoresist that was applied to the glass slide, and all of the components underwent a UV exposure at the required UV dosage (ABM Inc., San Jose, CA). Immediately following that, the slide was placed on the hot plate for a post-exposure bake for 1 min at 65 °C and an additional 4.5 min at 95 °C. It was then submerged in a SU-8 developer solution for a period of 8 min to remove the unwanted photoresist, the result of which is a positive mold of the microchannel or the so-called master.

The master of the microchannel was placed inside a Petri dish to allow for magnet positioning and liquid PDMS filling around the mold. The varying magnet configurations were created by changing the placement of two attracting Neodymium-Iron-Boron (NdFeB) permanent magnets (B222, $0.125'' \times 0.125'' \times 0.125''$, K&J Magnets, Inc.), named hereafter trapping magnets, with respect to the microchannel. This step required the utilization of holder magnets in the configuration shown in Fig. 1(a). A top row of four holding magnets (two B224 magnets, $0.125'' \times 0.125'' \times 0.25''$, K&J Magnets, Inc., on the ends and two B222 magnets in the center) and a bottom row of another four holding magnets (B441, $0.125'' \times 0.125'' \times 0.0625''$, K&J Magnets, Inc.) were used to complete the positioning of the trapping magnets. The bottom row of magnets was placed below the Petri dish holding the master.

The magnets were positioned under an inverted microscope (Nikon Eclipse TE2000U, Nikon Instruments, Lewisville, TX) with an attached CCD camera (Nikon DS-Qi1Mc). The gap between the trapping magnets is dependent on the holder magnet configuration utilized; therefore, the distance can be decreased with smaller holder magnets if possible. After the magnets were positioned, liquid PDMS, prepared by thoroughly mixing Sylgard 184 with the curing agent at a 10:1 ratio in weight, was distributed over the master in the Petri dish using a syringe until its free surface passed the interface between the top row of holder magnets and the trapping magnets. The dish was then placed in an isotemp vacuum oven (13-262-280 A, Fisher Scientific, Hampton, NH) for a 30 min degassing, and subsequently moved to a gravity convection oven (13-246-506GA, Fisher Scientific, Hampton, NH) for a curing period of 3 h at a temperature of 65 °C. After that, the holder magnets were carefully removed from the bottom of the Petri dish and the top of the trapping magnets as well. An additional layer of liquid PDMS was then placed onto the top surface of the cured PDMS in the dish for removing the indentation created

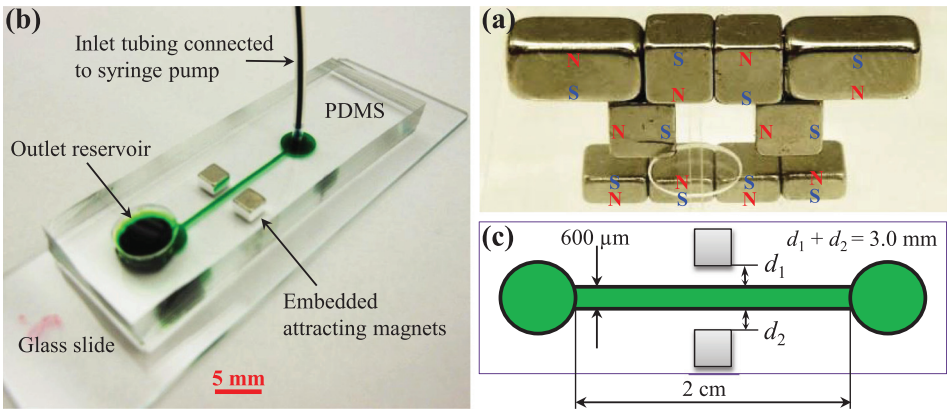

FIG. 1. Ferrofluidic microchip for diamagnetic particle concentration: (a) magnet configuration utilized to embed the two attracting permanent magnets into PDMS; (b) picture of the microfluidic chip with embedded trapping magnets; (c) configuration of the two trapping magnets for examining the effects of magnet asymmetry on diamagnetic particle concentration.

during the removal of the holder magnets. This treatment facilitated the visualization of fluid and particle motions in the microchannel.

After a second curing process, the completed channel was cut from the PDMS in the Petri dish with a scalpel and then carefully peeled away from the master to prevent damage and to facilitate the reuse of the mold. An exit reservoir was then punched into the PDMS slab along with a 0.047″ hole at the inlet for the attachment of tubing to facilitate the connection with a syringe pump. The channel side of the PDMS was then plasma treated (PDC-32 G, Harrick Scientific, Ossining, NY) for a period of 1 min along with an additional clean glass slide to create a hydrophilic surface. Once the PDMS slab and the treated glass slide were bonded together, a piece of polyethylene tubing compatible with a 25 gauge Luer stub was placed into the inlet hole. The opening with the attached tubing was sealed by placing the microchannel and tubing on a hot plate at 65 °C for 5 min. Afterwards, deionized water was pumped through the channel to prevent it from becoming hydrophobic before testing. A picture of the finished microfluidic chip with embedded trapping magnets (note they are attracting with opposite poles facing each other) is shown in Fig. 1(b).

B. Preparation of particle suspension in a ferrofluid

The diamagnetic particles utilized in the experiments were 5 μm-diameter green fluorescent polystyrene particles suspended in water with 1% solids. They were re-suspended in a water-based ferrofluid, denoted as EMG 408, acquired from Ferrotec (USA) Corporation. Originally, the ferrofluid consisted of 1.2% magnetic nanoparticles, with a diameter of 10 nm, by volume with a measured viscosity of 1.2 mPa s and saturation magnetization of 6.6 mTorr; however, it was diluted to 0.2× the original reported concentration using deionized water. Polystyrene particles were re-suspended in the diluted ferrofluid at a density of 2.0×10^6 particles/ml. TWEEN 20 (Thermo Fisher Scientific) was added to the particle suspension at a concentration of 0.1% by volume to facilitate the prevention of particle adhesions to the channel walls and other particles.

C. Experimental technique

A syringe pump (KDS 100, KD Scientific) was utilized to supply a constant volumetric flow rate through the microchannel. A 100 μl gas-tight glass syringe (SGE Analytical Science, Austin, TX) was used with a 25 gauge Luer stub tip to pump the ferrofluid solution through the polyethylene tubing connected to the inlet of the microfluidic chip. An inverted microscope imaging system (Nikon Eclipse TE2000U) was used to acquire videos and images in the particle trapping experiments presented below, which were then post-processed in the Nikon imaging software (NIS-Elements AR 2.30). The maximum ferrofluid flow rate for particle concentration was obtained by gradually reducing the flow rate from a large value at which all particles travelled through the microchannel region between the trapping magnets, to the one at which all particles started being trapped. To study the effects of magnet asymmetry on particle concentration, we varied the minimum magnet distances from the sides of the microchannel, i.e., d_1 and d_2 as highlighted in Fig. 1(c). The holder magnets utilized during our fabrication offered a distance of 3.6 mm between the inner faces of the two trapping magnets. This resulted in a fixed value of $d_1 + d_2 = 3.0$ mm as indicated in Fig. 1(c). Specifically, we varied d_1 from 0.4 mm to 0.7 mm and 1.5 mm, where the trapping magnets have an asymmetric configuration in each of the former two cases and have a symmetric configuration in the last case.

III. THEORY

A. Diamagnetic particle trapping mechanism

The two attracting magnets in Fig. 1 can confine the majority of the magnetic field lines within their attracting polar surfaces. Therefore, as seen from the magnetic field contour (the background color, the darker the larger strength) in Fig. 2, strong magnetic fields are induced in the microchannel region between the two magnets, while outside this region, the magnetic field drops off rapidly (see part B below on how the magnetic field distribution was obtained in our theoretical model). This creates strong magnetic field gradients within the microchannel towards the magnets at both their

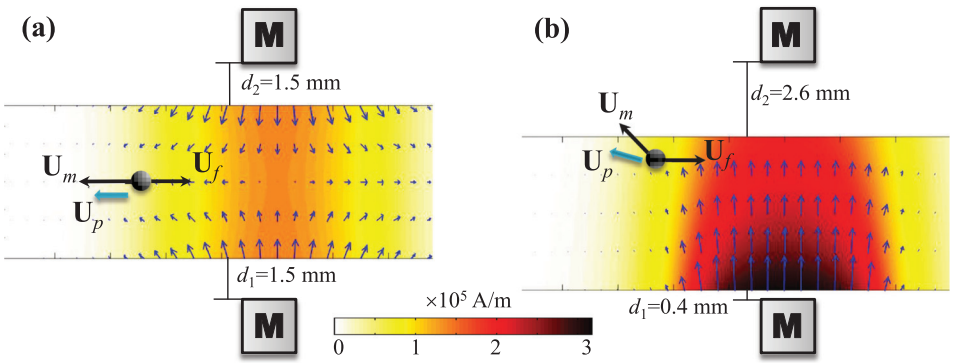

FIG. 2. Analysis of particle velocity, $\mathbf{U}_p$, for illustrating the mechanism of diamagnetic particle concentration in ferrofluid microflows (not drawn to scale): (a) symmetric magnet configuration with $d_1 = d_2 = 1.5$ mm; (b) asymmetric magnet configuration with $d_1 = 0.4$ mm and $d_2 = 2.6$ mm. In both cases, the background color shows the magnetic field contour (the darker color, the larger magnitude) in the horizontal plane of the microchannel, and the thin arrows display the vector distribution of the magnetic force experienced by particles. Particles are trapped in the locations where the magnetophoretic velocity, $\mathbf{U}_m$, counterbalances the local fluid velocity, $\mathbf{U}_f$.

front and rear edges. Since diamagnetic particles undergo negative magnetophoresis in ferrofluids,[31–34] they move against the magnetic field gradient and stay away from the magnets. As indicated by the analysis of particle velocity, $\mathbf{U}_p$, in Fig. 2, the negative magnetophoretic motion, $\mathbf{U}_m$, directs particles across fluid streamlines and up the flow. Therefore, the particles will be trapped in front of the magnets at the locations where the axial component of $\mathbf{U}_m$ can counterbalance the local flow velocity of the suspending ferrofluid, $\mathbf{U}_f$, leading to a continuous concentration.

The magnet asymmetry has a significant impact on the magnetic field distribution inside the microchannel between the facing surfaces of the two trapping magnets. It can be observed in Fig. 2(a) that the symmetric magnet configuration produces a symmetric magnetic field about the centerline of the microchannel. In contrast, the magnetic field distribution is asymmetric in the microchannel with an asymmetric magnet configuration, where the strength is apparently larger on the side of channel closest to the magnet as shown in Fig. 2(b). Therefore, introducing asymmetry results in an overall greater magnitude of magnetic field in the microchannel and hence a stronger magnetic force (see the force vector distribution in the form of arrows in Fig. 2). The induced magnetophoretic velocity, $\mathbf{U}_m$, directs particles towards the center and the sidewall of the microchannels with the symmetric and asymmetric magnet configurations, respectively, where particles can get trapped if the axial component of $\mathbf{U}_m$ counterbalances the local ferrofluid flow, $\mathbf{U}_f$. Note that particles are also deflected towards the bottom wall of the microchannel in both cases due to the magnetic field gradients formed in the channel depth direction.

B. Theoretical modeling of diamagnetic particle motion

A three-dimensional theoretical model was developed to simulate the transport and trapping of diamagnetic particles in ferrofluid flow through the straight rectangular microchannel under the influence of two trapping magnets. The center position of a diamagnetic particle, $\mathbf{r}_p$, was obtained by integrating over time the particle velocity, $\mathbf{U}_p = \mathbf{U}_f + \mathbf{U}_m$ (see Fig. 2)

$$\mathbf{r}_p = \mathbf{r}_0 + \int_0^t \left[\mathbf{U}_f(t') + \mathbf{U}_m(t')\right] dt', \tag{1}$$

where $\mathbf{r}_0$ is the initial position of the particle center and t is the time coordinate. The buoyancy and inertial effects on particle velocity are both excluded in Eq. (1) because the particle density is approximately the same as the ferrofluid density and the Reynolds number is small under the experimental conditions (0.08–0.2).[35–38] The ferrofluid flow, $\mathbf{U}_f$, in the microchannel was assumed to be fully developed and not affected by the particle motion. Hence, the flow velocity was expressed by the analytical formula for pressure-driven flow in a rectangular channel, which can be found in many fluid mechanics textbooks and are thus skipped here. The volumetric flow rate involved in the formula was determined by the electronic display of the syringe pump.

The magnetophoretic particle velocity, $\mathbf{U}_m$, is expressed by[39]

$$\mathbf{U}_m = \frac{-\mu_0 \phi a^2}{9\eta f_D} \frac{M_d L(\alpha) \nabla \mathbf{H}^2}{H}, \tag{2}$$

$$L(\alpha) = \coth(\alpha) - \frac{1}{\alpha}, \tag{3}$$

$$\alpha = \frac{\pi \mu_0 M_d H d^3}{6 k_B T}, \tag{4}$$

where μ_0 is the permeability of free space, ϕ is the volume fraction of magnetic nanoparticles in the ferrofluid, a is the radius of diamagnetic particles, η is the viscosity of the ferrofluid, f_D is the drag coefficient representing the interactions between a particle and a microchannel wall,[35–39] M_d is the saturation moment of the magnetic nanoparticles of the ferrofluid, $\mathbf{H}$ is the magnetic field vector with a magnitude of H, $L(\alpha)$ is the Langevin function with α being the ratio of the Zeeman energy of magnetic nanoparticles in the ferrofluid to the thermal energy of the nanoparticles,[40] d is the nominal diameter of the magnetic nanoparticles in the ferrofluid, k_B is Boltzmann's constant, and T is the temperature of the ferrofluid. Equation (2) indicates that the particle trapping performance increases with the ferrofluid concentration, ϕ, and the diamagnetic particle size, a. The magnetic field, $\mathbf{H}$, was obtained by superimposing that of the two trapping magnets, which was each computed from Furlani's analytical model.[41] Note that the fluid velocity, $\mathbf{U}_f$, and magnetophoretic velocity, $\mathbf{U}_m$, in Eq. (1) are both dependent on particle position, and so vary with time during the particle migration. A user-defined MATLAB® script was utilized to simulate and plot the particle trajectory, which was described in detail in earlier works from our group[39,42] and is omitted here for brevity.

The maximum ferrofluid flow rate allowed for diamagnetic particle trapping was computed by iterating its value until a particle starting from any position over the channel cross-section at the inlet could not flow through the trapping region between the trapping magnets. As our theoretical model neglects the particle-fluid and particle-particle interactions, it is unable to simulate the dynamic development of the particle trapping process as illustrated in Fig. 4 later. Actually, the predicted ferrofluid flow rate from our model represents only the initial maximum flow rate for particle trapping. This quantity can, however, be compared directly with the experimentally obtained ferrofluid flow rate because the latter value was determined by reducing the flow rate to below which no particle escaping occurred (see Sec. II C). In other words, the experimental flow rate was recorded at the state that particle trapping was just initiated and no significant particle-fluid and particle-particle interactions were present.

IV. RESULTS AND DISCUSSION

Fig. 3 compares the experimentally recorded images for 5 μm diamagnetic particle concentration in microchannels with various magnet asymmetries at four different time instants. Note that the right edge of all these images lines up with the leading edge of the trapping magnets. For the symmetric magnet configuration with $d_1 = d_2 = 1.5$ mm in

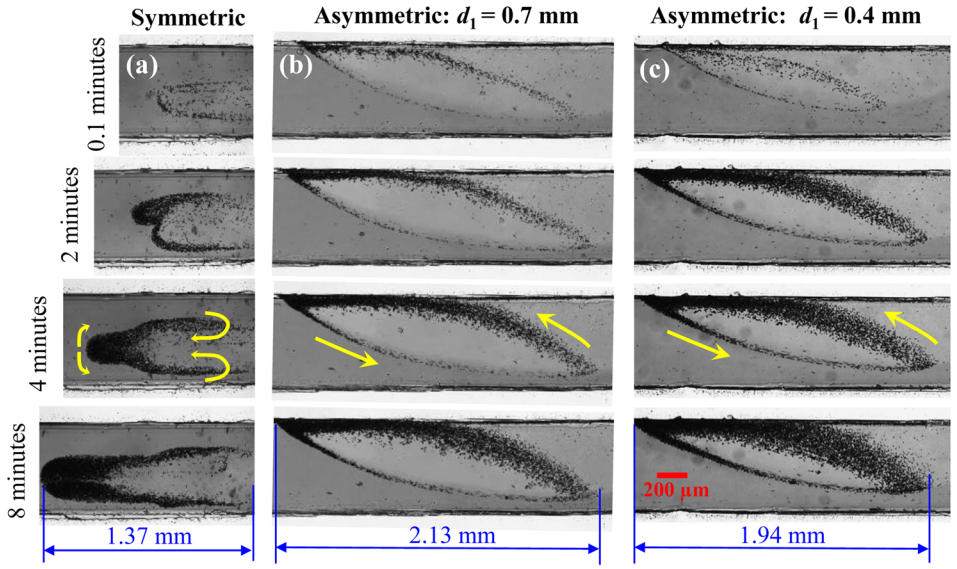

FIG. 3. Effects of magnet asymmetry on 5 μm diamagnetic particle concentration in 0.2 × EMG 408 ferrofluid at various times: (a) symmetric magnet configuration with $d_1 = d_2 = 1.5$ mm at a volumetric flow rate of 120 μl/h (or the average flow velocity is 1.65 mm/s); (b) asymmetric magnet configuration with $d_1 = 0.7$ mm and $d_2 = 2.3$ mm at a flow rate of 151 μl/h; (c) asymmetric magnet configuration with $d_1 = 0.4$ mm and $d_2 = 2.6$ mm at a flow rate of 207 μl/h. The arrows on the third row of images (i.e., 4 min) highlight the circulating directions of the concentrated particles. The dimensions on the bottom row of images indicate the length-wise size of the circulations. Note that the right edge of all images lines up with the leading edge of the trapping magnets. The flow direction is from left to right in all images.

Fig. 3(a), the complete trapping of particles occurs at a maximum volumetric flow rate of 120 μl/h, corresponding to an average flow velocity of 1.65 mm/s. It can be observed that the magnetic field gradients push particles towards the center of the channel where particle magnetophoresis overcomes the bulk fluid motion. Therefore, the particles progress upstream the channel until the bulk fluid velocity overcomes the magnetophoretic velocity. Once this occurs, the particles are pushed back towards the walls of the channel and repeat this motion creating nearly symmetric circulations as shown in Fig. 3(a). As time progresses, the trapped particle density increases and the circulations of the concentrated particles move towards the inlet of the microchannel. This is clearly demonstrated by the images recorded at a series of times in Fig. 3(a). The length-wise dimension of the circulations increases from 0.66 mm at 0.1 min to 1.37 mm at 8 min.

In contrast, single asymmetric circulation develops in the microchannel with an asymmetric magnet configuration, including $d_1 = 0.7$ mm & $d_2 = 2.3$ mm in Fig. 3(b) and $d_1 = 0.4$ mm & $d_2 = 2.6$ mm in Fig. 3(c). Moreover, a greater flow rate is achieved in both cases than in the microchannel with the symmetric magnet configuration. This enhanced particle trapping results from the increase in magnitude and gradient of the magnetic field inside the microchannel (see

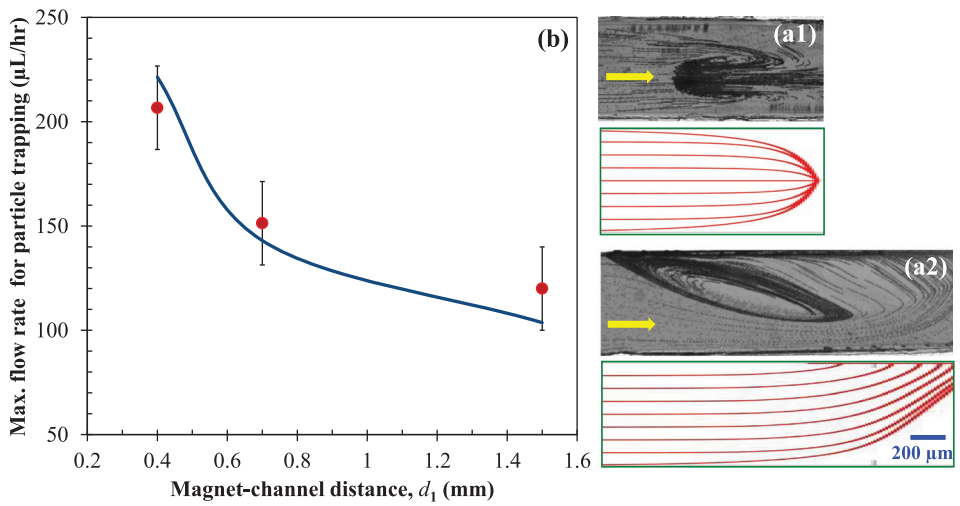

FIG. 4. Comparison of the experimental observations with theoretical predictions of 5 μm diamagnetic particle concentration in 0.2 × EMG 408 ferrofluid: (a1) and (a2) the composite images of particle trapping in the initial 5 s (top row in each panel) vs. predicted particle trajectories (bottom row in each panel) in the microchannels with the symmetric (a1) and the asymmetric ($d_1 = 0.4$ mm) magnet configurations (a2), respectively; (b) the experimentally (filled circles with error bars) and theoretically (solid line) obtained maximum flow rate for a complete particle trapping (i.e., all particles are trapped) vs. the magnet-channel distance, d_1. Note that the theoretical result in (a2) is truncated on the right side in order to match the position of the magnets in the experimental image. The block arrows indicate the bulk flow direction.

Fig. 2) due to the introduction of magnet asymmetry. Moreover, the asymmetric magnetic field pushes particles into the walls of the microchannel, such that the increased drag upon the particles also plays a part in increasing the trapping effectiveness. With either of the two asymmetric magnet configurations, particles travel towards the wall furthest from the magnet with the magnet-channel distance d_1 and meanwhile up the microchannel. Once the induced magnetophoretic velocity is surpassed by the local ferrofluid flow velocity, the particles are forced down the microchannel towards the magnets and away from the wall until the magnetophoretic motion again balances the fluid flow. This repetitive motion creates a counterclockwise circulation of concentrated particles shown in Figs. 3(b) and 3(c). Moreover, the location and dimension of this circulation remain nearly unchanged with time except for within the initial short period (less than 30 s). This trapping behavior is distinct from the continual moving-up and expansion of the particle concentration zone in the microchannel with the symmetric magnet configuration [see Fig. 3(a)].

In between the two asymmetric configurations, the more asymmetric of the magnets with respect to the microchannel, the greater flow rate is achieved for a complete diamagnetic particle trapping. Specifically, the maximum flow rate was determined to be 151 μl/h (or an average flow velocity of 2.09 mm/s) for the configuration with $d_1 = 0.7$ mm in Fig. 3(b), and 207 μl/h (or an average flow velocity of 2.86 mm/s) for that with $d_1 = 0.4$ mm in Fig. 3(c). However, the extent of magnet asymmetry does not seem to affect significantly the location and dimension of the particle circulation zone. It is observed from Figs. 3(b) and 3(c) that the less asymmetric magnet configuration with $d_1 = 0.7$ mm generates a little larger circulation with a length-wise dimension of 2.13 mm at 8 min as compared to 1.94 mm for the configuration with $d_1 = 0.4$ mm. However, the circulation in the latter case is slightly further away from the leading edge of the trapping magnets (which is at the right edge of the images illustrated) in both the stream-wise and cross-stream directions.

Fig. 4(a1) and 4(a2) compare the experimentally obtained composite images (top row in each panel, a superposition of 50 frames) of 5 μm diamagnetic particle concentration within the initial 5 s and the theoretically predicted particle trajectories (bottom row in each panel) in the microchannels with the symmetric (a1) and the asymmetric (a2) magnet configurations. Only the asymmetric configuration with $d_1 = 0.4$ mm is shown here as the results for the channel with $d_1 = 0.7$ mm are visually similar. The theoretical predictions are obtained for a complete particle trapping at the maximum flow rate, whose values (solid line) are compared with the experimental measurements (filled circles with error bars) in Fig. 4(b). We notice that the trajectories of particles prior to being trapped are qualitatively simulated by the theoretical model. However, no circulation is predicted for the trapped particles because only single particle motion is tracked in our model with no account of the particle-particle and particle-fluid interactions. These interactions become very strong when many particles are trapped and concentrated. We are currently developing a numerical model to take them into consideration for understanding and simulating the particle circulation. In addition, as we have explained in Sec. III B, the theoretically predicted maximum flow rates for particle trapping appear to agree reasonably with the experimental data in Fig. 4(b).

V. CONCLUSIONS

We have conducted an experimental and theoretical study of the effects of magnet asymmetry on the continuous concentration of 5 μm diamagnetic particles in ferrofluid flow through a straight rectangular microchannel. Two attracting permanent magnets are embedded into the PDMS of the ferrofluidic microchip with a fixed distance. Each magnet is placed on one side of the microchannel with either a symmetric or an asymmetric configuration, in which distinct circulation patterns of concentrated particles have been observed. It is also found that positioning the magnets around a microchannel asymmetrically increases the flow rate for particle concentration. Moreover, the maximum flow rate at which particles can be trapped increases as the asymmetry of the magnets about the microchannel increases. These effects of magnet asymmetry on the flow rate of particle trapping can be reasonably predicted by the theoretical model. However, the current model is unable to simulate the formation of circulation of concentrated particles due to the lack of consideration of the particle-fluid and particle-particle interactions.

ACKNOWLEDGMENTS

This work was supported by NSF under Grant No. CBET-1150670 (Xuan) and by Clemson University through Honors Undergraduate Research Program and Creative Inquiry Program (Xuan).

[1]A. Karimi, S. Yazai, and A. M. Ardekani, Biomicrofluidics **7**, 021501 (2013).
[2]J. Nilsson, M. Evander, B. Hammarstrom, and T. Laurell, Anal. Chim. Acta **649**, 141–157 (2009).
[3]R. M. Johann, Anal. Bioanal. Chem. **385**, 408–412 (2006).
[4]M. N. Hamblin, J. Xuan, D. Maynes, H. D. Tolley, D. M. Belnap, A. T. Woolley, M. Lee, and A. R. Hawkins, Lab Chip **10**, 173–178 (2010).
[5]D. Juncker, H. Schmid, and E. Delamarche, Nature Mater. **4**, 622–628 (2005).
[6]S. Zheng, H. K. Lin, B. Lu, A. Williams, R. Datar, R. J. Cote, and Y. C. Tai, Biomed. Microdevices **13**, 203–213 (2011).
[7]A. Kumar, J. S. Kwon, S. J. Williams, N. G. Green, N. K. Yip, and S. T. Wereley, Langmuir **26**, 5262–5272 (2010).
[8]Y. Zhang, H. Lei, Y. Li, and B. Li, Lab Chip **12**, 1302–1308 (2012).
[9]T. Ohta, P. Y. Chiou, and M. C. Wu, J. Microelectromech. Syst. **16**, 491–499 (2007).
[10]A. Kayani, K. Khoshmanesh, S. A. Ward, A. Mitchell, and K. Kalantar-Zadeh, Biomicrofluidics **6**, 031501 (2012).
[11]B. Hammarström, M. Evander, H. Barbeau, M. Bruzelius, J. Larsson, T. Laurell, and J. Nilsson, Lab Chip **10**, 2251–2257 (2010).
[12]J. Shi, D. Ahmed, X. Mao, S. S. Lin, and T. J. Huang, Lab Chip **9**, 2890–2895 (2009).
[13]R. Pethig, Biomicrofluidics **4**, 022811 (2010).
[14]B. H. Lapizco-Encinas and M. Rito-Palmomares, Electrophoresis **28**, 4521–4538 (2007).
[15]C. Church, J. Zhu, G. Huang, T. R. Tzeng, and X. Xuan, Biomicrofluidics **4**, 044101 (2010).
[16]N. Lewpiriyawong, C. Yang, and Y. Lam, Microfluid. Nanofluid. **12**, 723–733 (2012).

[17]A. Salmanzadeh, M. B. Sano, R. C. Gallo-Villanueva, P. C. Roberts, E. M. Schmelz, and R. V. Davalos, Biomicrofluidics **7**, 011809 (2013).
[18]N. Pamme, Lab Chip **6**, 24–38 (2006).
[19]M. Suwa and H. Watarai, Anal. Chim. Acta **690**, 137–147 (2011).
[20]N. T. Nguyen, Microfluid. Nanofluid. **12**, 1–16 (2012).
[21]N. Pamme, Curr. Opin. Chem. Biol. **16**, 436–443 (2012).
[22]Q. Ramadan and M. A. M. Gijs, Microfluid. Nanofluid. **13**, 529–542 (2012).
[23]S. K. Fateen, "Magnetophoretic focusing of submicron particles dispersed in a polymer-stabilized magnetic fluid," Ph.D. dissertation (MIT, 2002).
[24]E. Feinstein and M. Prentiss, J. Appl. Phys. **99**, 064901 (2006).
[25]R. M. Erb and B. B. Yellen, J. Appl. Phys. **103**, 07A312 (2008).
[26]A. R. Kose and A. Koser, Lab Chip **12**, 190–196 (2012).
[27]A. Winkleman, K. L. Gudiksen, D. Ryan, and G. M. Whitesides, Appl. Phys. Lett. **85**, 2411–2413 (2004).
[28]S. A. Peyman, E. Y. Kwan, O. Margarson, A. Iles, and N. Pamme, J. Chromatogr. A **1216**, 9055–9062 (2009).
[29]M. D. Tarn, S. A. Peyman, and N. Pamme, RSC Adv. **3**, 7209–7214 (2013).
[30]J. Zeng, C. Chen, P. Vedantam, T. R. Tzeng, and X. Xuan, Microfluid. Nanofluid. **15**, 49–55 (2013).
[31]T. Zhu, F. Marrero, and L. Mao, Microfluid. Nanofluid. **9**, 1003–1009 (2010).
[32]T. Zhu, R. Cheng, and L. Mao, Microfluid. Nanofluid. **11**, 695–701 (2011).
[33]L. Liang and X. Xuan, Microfluid. Nanofluid. **13**, 637–643 (2012).
[34]L. Liang and X. Xuan, Biomicrofluidics **6**, 044106 (2012).
[35]T. Zhu, D. J. Lichlyter, M. A. Haidekker, and L. Mao, Microfluid. Nanofluid. **10**, 1233–1245 (2011).
[36]T. Zhu, R. Cheng, S. A. Lee, E. Rajaraman, M. A. Eiteman, T. D. Querec, E. R. Unger, and L. Mao, Microfluid. Nanofluid. **13**, 645–654 (2012).
[37]J. Zeng, C. Chen, P. Vedantam, V. Brown, T. R. Tzeng, and X. Xuan, J. Micromech. Microeng. **22**, 105018 (2012).
[38]J. Zeng, Y. Deng, P. Vedantam, T. R. Tzeng, and X. Xuan, J. Magn. Magn. Mater. **346**, 118–123 (2013).
[39]L. Liang, J. Zhu, and X. Xuan, Biomicrofluidics **5**, 034110 (2011).
[40]R. E. Rosensweig, Annu. Rev. Fluid. Mech. **19**, 437–463 (1987).
[41]E. P. Furlani, *Permanent Magnet and Electromechanical Devices: Materials, Analysis and Applications* (Academic Press, New York, 2001).
[42]J. Zhu, L. Liang, and X. Xuan, Microfluid. Nanofluid. **12**, 65–73 (2012).